

Comparison Between Results of Quench Simulation and Tests of a 13 T REBCO Coil in a Strong Background Magnetic Field

Andrew V. Gavrilin , Ernesto S. Bosque , William S. Marshall , Kwangmin Kim, Dylan J. Kolb-Bond , Peng Xu , Iain R. Dixon , Yu Suetomi , Mark D. Bird , and Hongyu Bai 

Abstract—In the framework of the 40 T all-superconducting magnet project at the National High Magnetic Field laboratory, improvements have been made in a quench model and the quench code that has been constructed to simulate the behavior of a magnet consisting of an HTS inner coil set with an LTS background field. The quench model, initially developed for the NHMFL 32 T magnet project, incorporates additional details of the REBCO conductor on a localized level. These include nonuniform magnetic field distribution across each conductor turn and deformation of the turns due to screening currents which affects the true field angle applied to the conductor’s a-b plane. Detailed measurements of the test coil’s conductors have also been made to improve the simulations. These include the slope of the a-b plane using X-ray techniques and I_C (B, θ, T) of each conductor length using torque magnetometry. The test coil generating a field up to 13 T is an insulated, two-in-hand REBCO coil with twelve modules. Deliberate quench tests were performed with it in self-field and with a 11.4 T background field. The results and discussion of the comparisons are presented.

Index Terms—Critical current, magnetic field angle, quench protection, quench analysis, REBCO coil, screening current induced deformation, ultra-high field superconducting magnet.

I. INTRODUCTION

AS is well known, a reliable system for protecting a modern high-field REBCO magnet in the event of a quench is the most important component of the entire magnetic system. Within

Manuscript received 5 October 2023; revised 13 December 2023; accepted 5 January 2024. Date of publication 6 February 2024; date of current version 28 February 2024. This work was supported in part by the National High Magnetic Field Laboratory, in part by National Science Foundation under Cooperative Agreements Grant DMR-1644779, Grant DMR-1938789, and Grant DMR-2131790; and in part by the State of Florida. (Corresponding author: Andrew V. Gavrilin.)

Andrew V. Gavrilin, Ernesto S. Bosque, William S. Marshall, Kwangmin Kim, Iain R. Dixon, Yu Suetomi, Mark D. Bird, and Hongyu Bai are with the National High Magnetic Field Laboratory, Tallahassee, FL 32310 USA (e-mail: gavrilin@magnet.fsu.edu; bosque@magnet.fsu.edu; wsmarshall@magnet.fsu.edu; kwangmin.kim@magnet.fsu.edu; dixon@magnet.fsu.edu; yu.suetomi@magnet.fsu.edu; bird@magnet.fsu.edu; bai@magnet.fsu.edu).

Dylan J. Kolb-Bond was with the National High Magnetic Field Laboratory, Tallahassee, FL 32310 USA. He is now with Commonwealth Fusion Systems, Devens, MA 01434 USA (e-mail: kolbbond@gmail.com).

Peng Xu was with the National High Magnetic Field Laboratory, Tallahassee, FL 32310 USA. He is now with Brookhaven National Laboratory, Upton, NY 11973 USA (e-mail: pxu@bnl.gov).

Color versions of one or more figures in this article are available at <https://doi.org/10.1109/TASC.2024.3362762>.

Digital Object Identifier 10.1109/TASC.2024.3362762

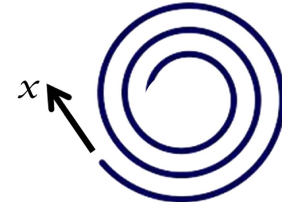


Fig. 1. Schematic of a pancake winding and the coordinate system.

the NHMFL 40 T magnet project [1], the main tool for developing the detection and protection systems is accurate computer simulation, which involves the use of comprehensive simulation model of the processes governing the quench behavior.

The basic model [2], [3] was developed as part of the 32 T magnet project [4], [5], [6], a development of which is the 40 T magnet program. In this work, this model was significantly supplemented by taking the effect of screening currents [7] into account and then tested by comparing the results of experiments on test coils, deliberate quenches by simultaneously fired quench protection heaters, with the calculation results.

II. NUMERICAL SIMULATION PROCEDURE

The approach to modeling of the thermal part of the problem is based upon consideration of a pancake winding as a discrete structure: a REBCO tape-wound flat spiral, a “disk”. Two disks connected at the inner diameter form a double pancake/module, whereas the modules are connected at the outer diameter that enables one to model a 3D normal zone propagation. The coordinate axis, x , follows the conductor spiral path (Fig. 1), i.e., aligned with the conductor. The corresponding heat conduction equation with the heat term is as follows (in W/m):

$$(A_{Cu}C_{Cu} + A_{sc}C_{sc} + A_{ins} (C_{ins} + f\gamma_p^{He}c_p^{He})) \frac{\partial T(x, t)}{\partial t} = \frac{\partial}{\partial x} \left\{ A_t k_t \frac{\partial T}{\partial x} \right\} + (A_t Q_J + A_t Q_{AC}) + \sum_{i=1}^4 \frac{P_i}{\delta_i} k_i^{(ins)} \left(T_i^{(ins)} \right) (T_i - T) + P_{1.2} Q_{heater}, \quad (1)$$

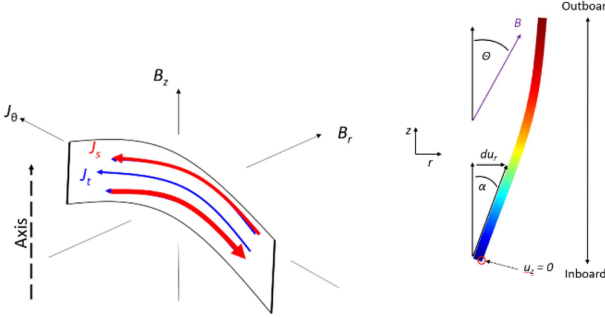


Fig. 2. Diagram of a single turn fragment of superconductor. The transport current and screening supercurrents are shown.



Fig. 3. Segmented REBCO tape cross-section.

$T = T(x, t)$ is the tape temperature, $A_t = A_{Cu} + A_{sc}$ is the tape cross-section area, which is a sum of copper matrix and non-copper portion cross-section areas. $A_{Cu}C_{Cu} + A_{sc}C_{sc} + A_{ins}(C_{ins} + f\gamma_p^{He}c_p^{He})$ is the insulated tape heat capacity, in $\text{J}/(\text{m K})$, which also includes the heat capacity of helium in the winding at constant pressure; f is the helium proportion of the insulation in terms of volume. The helium density γ_p^{He} is considered temperature dependent to mimic the helium vaporization process. The second term on the right side of the equation includes Joule heating, index heating during the transition to the normal state, and heating due to AC losses [6] owing to the effect of screening currents. The penultimate term serves to describe the transverse heat transfer, radially within a given pancake and axially between the adjacent disks, P is the contact perimeter, and δ is the insulation thickness. The last term is the heat influx from the quench protection heaters installed between the modules.

The index and Joule power densities are calculated using the following model:

If $I < I_C(B, T, \theta)$, then $A_t Q_J = IE = IE_0 i^{n(T, I)}$, $i = I/I_C$. If $I \geq I_C(B, T, \theta)$ and $\partial E/\partial I \approx (E - E_0)/(I - I_C) < \rho_{Cu}/A_{Cu}$, then $A_t Q_J = I E$.

Else, i.e., $\partial E/\partial I \geq \rho_{Cu}/A_{Cu}$, $A_t Q_J = I(I - I_C)\rho_{Cu}/A_{Cu}$, if $I_C > 0$. Finally, $A_t Q_J = I^2 \rho_{Cu}/A_{Cu}$, if $I_C = 0$.

The dependence of I_C on the magnetic field magnitude, B , and field angle, θ , to the ab-plane is suggested in the NHMFL [8]. Recently, the I_C -measurements were carried out at several temperatures in the range of interest that enabled one to obtain the temperature dependence as well: we plan to publish the results in one of our next articles.

The field angle, θ , is the superposition / algebraic sum of (a) the angle between the magnetic field vector and the coil axis, Z , (b) the rotation angle due to the screening currents (the rotation is actually bending, Fig. 2) [7], [9] and (c) “the offset” that is the deviation of the YBCO ab-plane from the ideal position, which is typically around ± 2 deg., also measured.

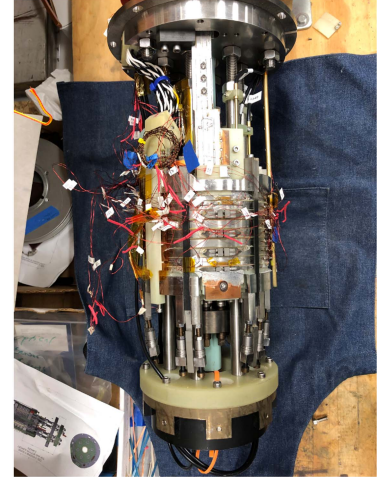


Fig. 4. Test coil assembly.

However, since the tape is wide, the spatial distributions of field angle and magnetic field magnitude across it turn out to be non-uniform. In order to include this phenomenon appropriately, each turn is broken in several segments (parallel resistances, Fig. 3) instead of using the turn-average or “effective” values of the field and field angle. Dynamically, there may be both quenched and not-quenched-yet segments of a given turn.

Obviously, when the turn quenches, its rotation and bending should disappear, which was simulated using the following approach. We assume that the rotation angle $\alpha \sim (I_C - I)B_R B_Z$, where B_R and B_Z are radial and axial components of the magnetic field, respectively. Using the rotation angle matrix at full field, $\alpha_0(x, z) = C(x, z)(I_C(x, z) - I_0)B_R(x, z)B_Z(x, z)$, one calculates the matrix of coefficients $C(x, z) = \alpha_0 / [(I_C - I_0)B_R B_Z]$, which are assumed to be fixed. Then, when and if the coil current decays and the critical current changes with time, one recalculates the rotation angle matrix, $\alpha(x, z, t) = C(x, z)(I_C(x, z, t) - I(t))B_R(x, z, t)B_Z(x, z, t)$, until it is reset to zero.

The rotation of the turns occurs in such a way that they try to align with the magnetic field lines, increasing the critical current and thus lengthening the heating time of the winding by quench protection heaters before quench.

III. SIMULATION RESULTS AND DISCUSSIONS

The test coil known as Test Coil 2 (TC2) on which the experiments were carried out is assembled from 12 modules, wound with a bundle, consisting of two SuperPower REBCO tapes and a high RRR copper co-wind 127 μm thick, along with stainless steel co-wind (Fig. 4).

The coil winding inner diameter is 40 mm, the outer one is 140 mm. The conductor and steel cowind are properly graded to reduce the strain down to acceptable level. There are 11 doubled quench protection heaters (22 totally) installed between the modules. Each heater covers uniformly 70% of the surface of its pancake. The heating power is graded to have more power in the middle of the coil, where the critical current is higher due

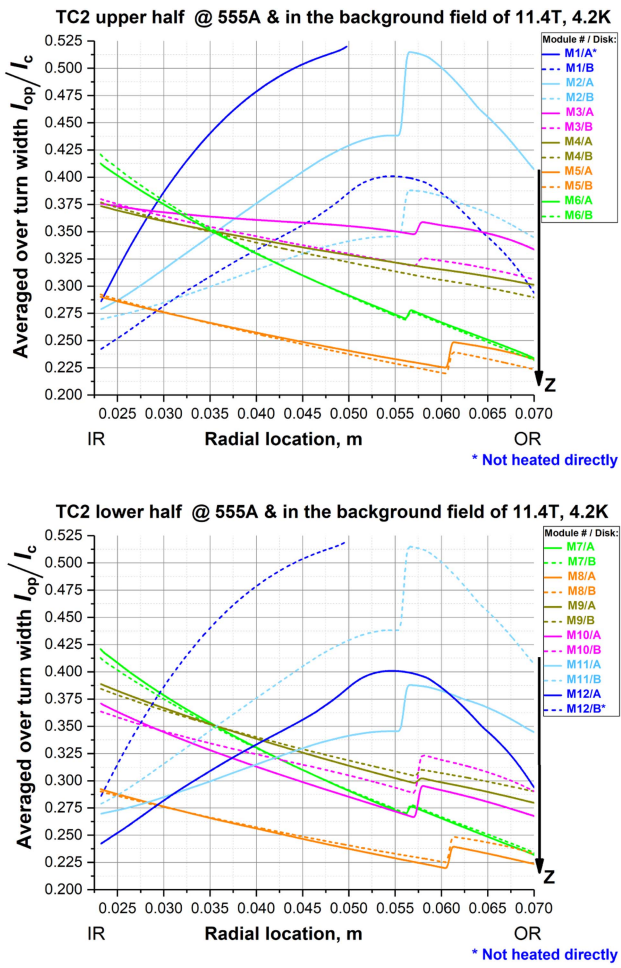


Fig. 5. Distribution of the critical current fraction in TC2 throughout the disks at full field. Numbering of modules and pancakes: M1/A and M1/B are pancakes belonging to the same module 1 (M1). M1 is located at the coil bottom, and M12 is positioned at the top.

to the smallness of the radial component of magnetic field. The average heating power was around 6 W per meter of the bundle. The coil was tested in a fixed background magnetic field of 11.4 T, which made it possible to obtain 26.2 T in the winding at 555 A. The critical current dependence on magnetic field, field angle and temperature were measured and thus well known for each tape used in the coil. The rotation angle matrix at full field was calculated using our COMSOL model [7], [9].

As can be inferred from Fig. 5, the safety margin was quite large (the coil operated at $\sim 52\%$ of I_C), and there are the lead-ins and lead-outs in which the second tape is a different one in the modules, i.e., there are internal joints: the stepwise leaps are explained by this fact. The quench protection heaters, fired simultaneously, turned out to be powerful enough to reliably and quickly quench the coil, as predicted, using a 600 ms long pulse of current.

The TC2 current discharge duration and module voltage magnitudes and profiles are very comparable to the test plan prediction (Fig. 6). The calculated and measured current decay patterns are practically identical. The calculated and measured

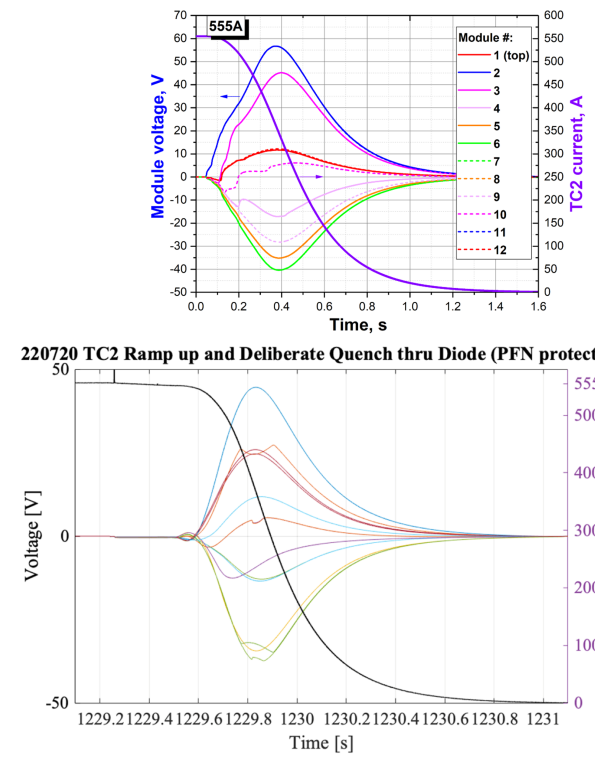


Fig. 6. Calculated (upper plot) and measured (lower plot) coil current and module voltages during a deliberate quench.

voltages across the modules differ slightly in magnitude (by about 10%) and shape. In fact, this was the first time that all inputs were fairly well known, and so some success has finally come.

IV. CONCLUSION

An approach for creating comprehensive simulation models of a quench in a HTS insulation coil wound with a REBCO coated conductor has been proposed. The validity of the methodology has been proven by comparison of experimental results on a large enough test coil with calculations.

REFERENCES

- [1] H. Bai et al., "The 40 T superconducting magnet project at the national high magnetic field laboratory," *IEEE Trans. Appl. Supercond.*, vol. 30, no. 4, Jun. 2020, Art. no. 4300405.
- [2] A. V. Gavrilin et al., "Comprehensive quench analysis of the NHMFL 32T all-superconducting magnet system," in *CHATS on Applied Superconductivity*. Bologna, Italy: Univ. Bologna, Sep. 14-16, 2015. Accessed: Feb. 12, 2024. [Online]. Available: https://indico.cern.ch/event/372812/contributions/1792178/attachments/1158596/1667005/19_Gavrilin.pdf
- [3] A. V. Gavrilin and H. W. Weijers, "Comprehensive modelling study of quench behaviour of the NHMFL 32 T all-superconducting magnet system. Input data and methodology aspects," in *Proc. 5th Int. Workshop Numer. Modelling High Temp. Supercond.*, Jun. 15-17, 2016. Accessed: Feb. 12, 2024. [Online]. Available: <http://www.die.ing.unibo.it/pers/morandi/didattica/Temporary-HTSModelling2016/Gavrilin.pdf>
- [4] H. W. Weijers et al., "Progress in the development and construction of a 32-T superconducting magnet," *IEEE Trans. Appl. Supercond.*, vol. 26, no. 4, Jun. 2016, Art. no. 4300807, doi: [10.1109/TASC.2016.2517022](https://doi.org/10.1109/TASC.2016.2517022).
- [5] L. Cavallucci, M. Breschi, P. L. Ribani, A. V. Gavrilin, H. W. Weijers, and P. D. Noyes, "A numerical study of quench in the NHMFL 32 T magnet,"

IEEE Trans. Appl. Supercond., vol. 29, no. 5, Aug. 2019, Art. no. 4701605, doi: [10.1109/TASC.2019.2900175](https://doi.org/10.1109/TASC.2019.2900175).

[6] A. V. Gavrilin, J. Lu, H. Bai, D. K. Hilton, W. D. Markiewicz, and H. W. Weijers, “Observations from the analyses of magnetic field and AC loss distributions in the NHMFL 32 T all-superconducting magnet HTS insert,” *IEEE Trans. Appl. Supercond.*, vol. 23, no. 3, Jun. 2013, Art. no. 4300704, doi: [10.1109/TASC.2013.2244154](https://doi.org/10.1109/TASC.2013.2244154).

[7] D. Kolb-Bond et al., “Screening current rotation effects: SCIF and strain in REBCO magnets,” *Supercond. Sci. Technol.*, vol. 34, no. 9, 2021, Art. no. 095004, doi: [10.1088/1361-6668/ac1525](https://doi.org/10.1088/1361-6668/ac1525).

[8] J. Jaroszynski et al., “Rapid assessment of REBCO CC angular critical current density J_c (B , $T = 4.2$ K, θ) using torque magnetometry up to at least 30 T,” *Supercond. Sci. Technol.*, vol. 35, no. 9, 2022, Art. no. 095009, doi: [10.1088/1361-6668/ac8318](https://doi.org/10.1088/1361-6668/ac8318).

[9] Y. Suetomi et al., “Screening current induced stress/strain analysis of high field REBCO coils with co-winding or over-banding reinforcement,” *IEEE Trans. Appl. Supercond.*, vol. 34, no. 5, Aug. 2024, Art. no. 8400206.